
Introductory Lecture

Time-resolved chemistry at atomic resolution

Philip Coppens* and Irina V. Novozhilova

*Department of Chemistry, State University of New York at Buffalo, Buffalo,
NY 14260-3000, USA*

Received 19th July 2002, Accepted 19th July 2002

First published as an Advance Article on the web 8th October 2002

Though time-resolved studies are still at an early stage, the field is rapidly being developed and applied to an increasingly broad spectrum of problems with timescales varying from seconds or more down to femtoseconds. In this overview a number of different techniques are discussed, with emphasis on chemical applications in which information is obtained at the atomic level. The need to correlate with theory, both for calibration of theoretical methods and to obtain related information not accessible experimentally, is stressed.

Background

The importance of time-resolution in the study of a wide variety of chemical processes can hardly be overestimated. While molecular structure is a basic concept and must be known before a fundamental understanding can be reached, chemical processes are dynamic, and reaction pathways and their transition states play a crucial role in determining the products of chemical reactions.

Time-dependence in chemistry is implied in the century-old Arrhenius equation, which expresses the rate of a chemical reaction in terms of an activation energy in the exponent and a pre-exponential factor. More detailed understanding of the physics underlying the kinetics followed from the work of Polanyi and Wigner, Eyring, Karplus, Polanyi and Zewail and others. It soon became apparent that to follow rapid atom dynamics the existing experimental methods needed vast improvement, as motions of several ångströms are achieved in picoseconds or less, so that to reach a reasonable precision, time resolutions of femtoseconds are needed. The stopped flow kinetics widely applied in the forties have now been complemented by flash photolysis, and especially laser-triggering of photochemical reactions. The increasing time-resolution achieved in the past decades has been described by Zewail in his Nobel lecture as an experimental 'arrow of time', proceeding to ever shorter timescales.¹

Though studies of kinetic processes, and in particular vibrational energy transfer within molecules, are essential, the elucidation of time-dependent geometry changes remains one of the crucial requirements for the understanding of chemical dynamics. Examination of time-dependent geometry implies the study of transient species, intermediate in chemical processes. They are in general highly reactive and can be precursors in important chemical and biological processes. How far have we progressed in time-resolved structure determination and what are the prospects?

Time resolution

The concept of time-resolution implies that that time is sliced and that a direct image, scattering or diffraction pattern is recorded instantaneously, before significant changes occur. We will concentrate here on timescales of a millisecond or less, but note that this volume gives abundant evidence of the important information that can be provided by studying slower processes such as nucleation^{2,3} and crystallization,⁴ while slower-moving solid-state reactions⁵ must also be mentioned.

A distinction can be made between reversible processes, which can be repeated a very large number of times, and irreversible processes such as fast moving chemical reactions which can be measured only once along their path, because of read-out limitations of current detectors. However, such processes can be repeated with a different pump–probe delay time t , to give an image of the changes along the reaction path. Such methods have been applied with great success in time-resolved biochemical crystallography,^{6–8} and in a first study of a solid-state dimerization reaction reported in this volume.⁹ Alternatively, it may be possible to ‘stop the clock’ and stabilize an otherwise short-lived state by cooling. The trapped metastable state may correspond to a transient state under ambient conditions. Such freezing allows much longer periods of data collection, and thereby affords higher spatial resolution, thus providing important information not otherwise accessible. Examples of such studies are our diffraction and IR spectroscopy measurements on low-temperature metastable states of transition metal complexes with small ligands such as NO, N₂¹⁰ and SO₂,¹¹ and the trapping of short-lived intermediate species along the reaction pathway of the enzyme cytochrome P450cam.¹²

The stroboscopic technique, applicable to reversible processes, is intermediate between repeated measurement of different samples with different delay times and the study of trapped species. The stroboscopic technique is very well suited for the study of molecular triplet states, generated through intersystem crossing from the initially formed excited singlet states. They often have lifetimes of microseconds or more, especially at reduced temperatures. If the pump and probe pulses are sufficiently narrow, the stroboscopic technique can also be applied to faster reversible processes and the evolution with time followed by varying the delay time between the pump and the probe pulses in a series of runs. The observations are made in rapid succession, sometimes thousands of times per second on a single specimen. Measurements with pump-on conditions can be followed immediately (but within the limitations imposed by the detector read-out time) by measurement without the periodic pump pulses. Precise measurement of the intensity *change* has important advantages, as it eliminates variations in intensity from, for example, long-range beam instability and allows toleration of moderate sample decay, and thus increases the sensitivity of the method. In monochromatic single crystal diffraction studies, in which a large number of reflection intensities are to be measured, the light-on phase may consist of the recording of a single area-detector frame, followed immediately by the measurement of the same oscillation range under light-off conditions.

Geometry information from spectroscopic studies

a Geometric information derived from vibrational fine structure of the UV absorption and emission spectra

Franck–Condon analysis of the intensity and spacing of the vibrational fine structure of the UV and visible absorption and emission spectra (when resolved) allows determination of the distortion upon excitation, provided the vibrational spectrum is dominated by a single mode.^{13,14} The technique often gives information on one prominent distortion that occurs, as in a recent study of nitridorhenium complexes,¹⁵ and for binuclear Pt and Rh complexes as discussed in more detail below.

b Time-resolved Raman and IR studies

Pump–probe time-resolved IR and infrared spectroscopy are extremely useful in providing information on the rate and mechanism of photochemical reactions. New equipment development¹⁶ and commercial availability of the equipment is facilitating more widespread application. The results are in many ways complementary to those obtained by diffraction techniques, but can, through analysis of group frequency changes, be used to infer information on the strengths of bonds associated with identified frequencies, and thus indirectly on geometry changes.

c Time-resolved XAFS

Time-resolved X-Ray absorption fine-structure analysis (XAFS) has the great advantage that it can be performed in the condensed phase and at relatively low concentration, and is thus highly relevant for processes occurring under ambient conditions. The inner coordination sphere of the resonating atom is probed by analysis of the extended fine structure, while near edge features can give information on changes in oxidation state or coordination number that are taking place. The studies by Chen and coworkers on the transient intermediate produced by photoexcitation of nickeltetraphenyl porphyrin-piperidine₂,¹⁷ and on photooxidation and exciplex formation of Cu(I) (dmp)₂, reported at this conference,¹⁸ are the first examples of nanosecond timescale EXAFS experiments.

Amorphous phase vs. crystal diffraction experiments

Diffraction experiments in the gas phase pose major challenges because of the low number density of the molecules and the lack of the constructive interference typical of the scattering by periodic arrays. Nevertheless, a number of very high temporal resolution studies of chemical reactions have now been accomplished by ultrafast electron diffraction (UED). First among these is the iodine elimination reaction of 1,2-diiodotetrafluoroethane to give tetrafluoroethylene,¹⁹ and more recently the ring opening reaction of 1,3-cyclohexadiene.²⁰ In the latter case the pump laser beam was derived from the same laser that generates the electron beam.

The random orientation of the molecules in the gas phase necessarily limits the results to a radial distribution curve, which means that the method is suitable for not too complicated reactants, a condition also imposed by the need to achieve a reasonable vapor pressure. In the case of diiodotetrafluoroethane,¹⁹ the radial distribution difference function clearly shows non-concerted disappearance of the two C-I vectors in 17(2) ps, indicating a two-step iodine elimination, with an intermediate non-bridged radical state. The radial distribution function changes and their interpretation are shown in Fig. 1. Typically the *differences* between the light-on and light-off patterns are analyzed, a recurring theme in many of the time-resolved studies.

The ring opening of 1,3-cyclohexadiene to give 1,3,5-hexatriene is in some respects a more challenging experiment, as strongly-scattering heavy atoms are absent, analysis of light-on/light-off difference patterns becomes imperative. Changes in the interatomic vectors are clearly evident from the difference electron diffraction patterns, but the analysis of the time-resolved pattern is complicated by the fact that at least four different product structures, related by rotations around the C-C bonds must be considered.

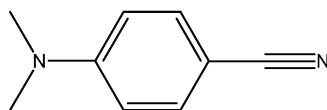
Time-resolved studies of processes in crystals have the great advantage that three-dimensional structural changes are accessible. In contrast with macromolecules, in which the active site is usually within the molecular envelope, in smaller unit cell crystals the molecular environment can play an active role. The advent of supramolecular crystallography allows incorporation of one type of guest molecule in a variety of host structures,²¹ and opens the possibility of using dilute, yet crystalline media.

While few chemically- rather than biologically-motivated solid-state diffraction studies have been reported so far, the number of studies may be expected to grow rapidly in the coming years. In both studies discussed in the following section information from other time-resolved techniques is available to complement the diffraction results.

Comparing information from parallel time-resolved techniques: two examples

a 4-(Dimethylamino) benzonitrile DMABN

In the molecule of DMABN a donor and acceptor group are linked by an aromatic ring.



4-(dimethylamino)benzonitrile

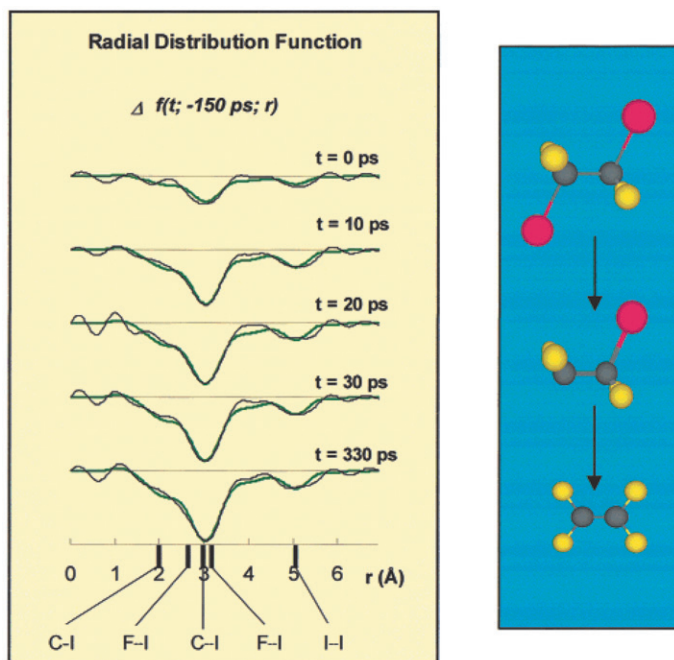


Fig. 1 Difference radial distribution function of diiodotetrafluoroethylene after excitation from time-resolved electron diffraction and interpretation. (Reprinted with permission from ref. 1. Copyright 2000 The American Chemical Society.)

The molecule is regarded as a typical example of a species in which intramolecular charge transfer (ICT) occurs on photoexcitation. In non-polar solvents DMABN shows a single fluorescence component in the UV, while in polar solvents an additional spectral component is observed in the visible region, corresponding to a highly polar ($\mu = 17$ D, compared with 6.7 D for the ground state²²) charge-separated singlet state. It is generally accepted that the latter is due to a 'twisted intramolecular charge transfer (TICT) state, though other models have been proposed. A shorter (S_0) and a longer lifetime (S_1) fluorescent state are observed. Picosecond transient IR measurements ruled out structures for the S_1 state in which the negative charge was confined to the phenyl ring, or the C–N(CH₃)₂ bond order increased.²³ Subsequent time-resolved resonance Raman measurements including D and ¹⁵N substitution,²⁴ indicated a 96 cm⁻¹ frequency downshift of the phenyl–N stretching vibration, which supports electronic decoupling of the amino and benzonitrile groups, and thus the twisted TICT model, but is not in agreement with the planar intramolecular charge transfer (PICT) model. The spectra further indicate sp³ pyramidal character of the dimethylamino substituent in the excited state. This is of interest as theoretical predictions of this distortion are frequently dependent on the level of theory used. A full optimization of the excited state structure was not available at the time the experimental work was reported.²⁴

The crystal experiment by Techert *et al.* used a powder sample with a room-temperature fluorescence lifetime of 1.9 ns.²⁵ The diffraction pattern shortly after excitation ($\sim 10^{-10}$ s) was refined to give an initial excited state population of 28–32%, and an increase in torsional angle around the exocyclic C–N bond from 0 to 10(1)°, thus confirming the TICT model. While the ground state molecule is slightly pyramidal at the amino nitrogen atom (the angle between NCC and benzene planes $\theta_{\text{inv}} = 13^\circ$ before excitation), the experiment indicates that the nitrogen atom becomes less inverted upon light induced charge transfer ($\theta_{\text{inv}} = 3^\circ$ at 80 ps). Interestingly, the relaxation time of the diffraction pattern of 520 ps is shorter than the electronic lifetime of the excited state as indicated by the fluorescence lifetime. This discrepancy suggests a complex mechanism before return to the ground state and requires further analysis.

In addition to the radiative decay of DMABN directly back to the ground state, intersystem crossing (ISC) occurs to a phosphorescing triplet state (³T₁), the structure of which has been

investigated by nanosecond resolution resonance Raman spectroscopy.²⁶ The results indicate the 3T_1 state to be a $\pi\pi^*$ charge-separated state of planar or near-planar structure, in agreement with the increased dipole moment of 12 D,²² and as predicted by several theoretical studies.

b The $[\text{Pt}_2(\text{pyrophosphate})_4]^{4-}$ ion (pyrophosphate, $(\text{H}_2\text{P}_2\text{O}_5)^{2-}$)

The Pt–Pt distance in the $[\text{Pt}_2(\text{pyrophosphate})_4]^{4-}$ (Ptpop) ion is bridged by four ligands in a paddlewheel type arrangement (Fig. 2). At room temperature, the $^3A_{2u}$ excited state has a lifetime of 9–10 μs in water and acetonitrile solutions, and a high quantum yield ($\phi_r = 0.5$ – 0.6) for phosphorescence.²⁷ As a result of spin–orbit coupling, the triplet level is split into two sub-levels: a lower-lying A_{1u} level, and a second E_u level $\sim 42\text{ cm}^{-1}$ higher in energy.²⁸ As the lower A_{1u} level has a much longer lifetime than the E_u level, at ambient temperature, at which the spacing is much smaller than kT , the phosphorescence is mostly from this state, while at very low temperatures (below $\approx 30\text{ K}$) the A_{1u} level with a lifetime of 6.06 ms dominates the emission process.²⁸ As a result, the lifetime is strongly temperature dependent in the region in which the 42 cm^{-1} splitting is comparable with kT , a feature that can be used for temperature calibration purposes.²⁹

Franck–Condon analysis of the vibrational fine structure of the absorption and emission spectra indicated a shortening of the Pt–Pt bond by 0.21 \AA (with an error estimated at 10–15%), based on the assumption that the spectrum is dominated by the metal–metal stretch.³⁰ In combination with the X-ray value of the ground state distance, this result corresponds to a Pt–Pt excited state bond length of 2.71 \AA . A second spectroscopic study based on Raman data and application of the empirical Badger’s rule, which relates a change in stretching frequency with a change in bond length, gives a value of 2.81 \AA for the excited state bond length.³¹ A time-resolved EXAFS study has also been reported. It gives a shortening of the Pt–phosphorus bond by 0.047(11) \AA , but the EXAFS curve is not sensitive to the longer Pt–Pt distance. To infer the gross molecular changes, the authors therefore used a spectroscopic excited state Pt–Pt distance of 2.75 \AA to derive a movement of 0.52(13) \AA of the planes through four P atoms attached to one platinum along the Pt–Pt axis.³²

The stroboscopic X-ray diffraction study was done at 17 K with a repeat frequency of 5000 Hz and a 33 μs X-ray pulse length, which may be compared with the 50 μs lifetime of the triplet state at 17 K. In the experiment sensitivity was enhanced by immediately following collection of a light-on frame with that of a light-off frame (Fig. 3).

Since the three-dimensional structure is refined in the single-crystal diffraction analysis, the light-induced structural change can be illustrated by a *photodifference* map,³³ obtained by Fourier summation with coefficients equal to the difference between the ‘on’ and ‘off’ structure factors. The photodifference map shows the *change* in electron density upon light exposure. The map (Fig. 4)

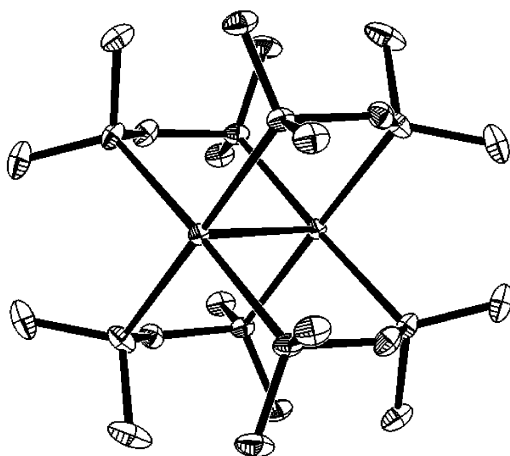


Fig. 2 ORTEP drawing of the $[\text{Pt}_2(\text{pyrophosphate})_4]^{4-}$ ion.

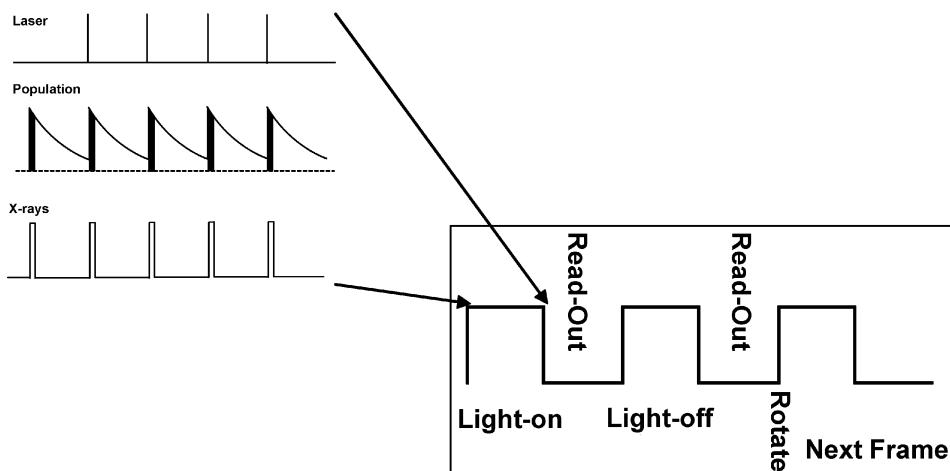


Fig. 3 Time structure and data collection strategy of the stroboscopic diffraction experiment.

gives clear evidence for a displacement of the Pt atoms in a direction towards the other Pt atom in the molecular ion and shows that the direction of the displacement does not coincide exactly with the intramolecular Pt–Pt vector, indicating that a small molecular rotation ($\approx 3^\circ$) accompanies the shortening of the Pt–Pt bond on excitation. Least-squares analysis of the response ratios, defined as $\eta = (I_{\text{on}} - I_{\text{off}})/I_{\text{off}}$,³⁴ gives a shortening of the Pt–Pt bond by 0.28(9) Å, in satisfactory agreement with the spectroscopic results. It must be emphasized that this time-resolved X-ray study is but a first result, that can be improved by the use of a more intense beam and smaller samples, the former

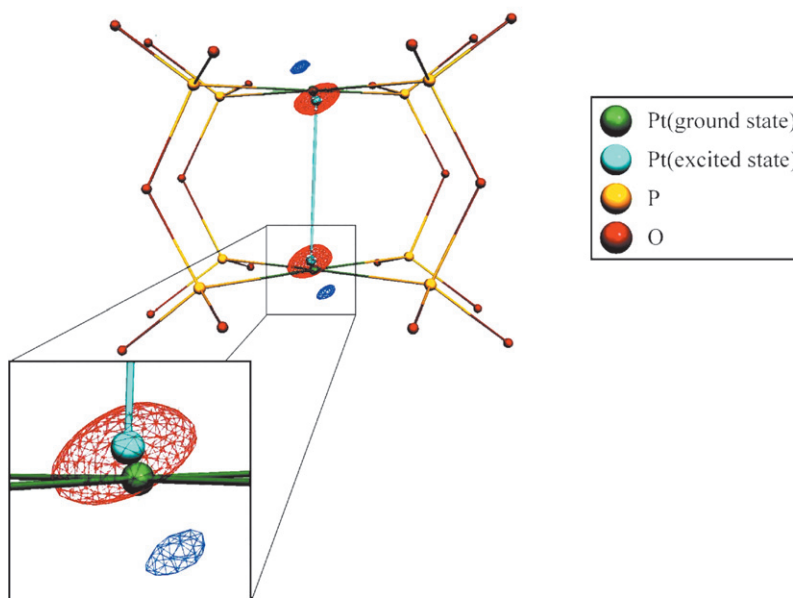


Fig. 4 Three-dimensional photodifference map along the Pt-Pt bond in the $[\text{Pt}_2(\text{pyrophosphate})_4]^{4-}$ ion.

to speed up data collection so that larger data sets can be collected before crystal damage becomes prohibitive, the latter to improve the photon/active-molecule ratio to obtain larger conversion percentages in the crystal than achieved in the first experiment ($2.0 \pm 0.1\%$).

All studies agree on the contraction of the molecule, which theoretical calculations discussed in the following section attribute to a transition of an electron from a $5d\sigma^*$ Pt–Pt antibonding orbital to a $6p\sigma$ orbital, which is bonding with regard to the Pt–Pt interaction.

The interplay between theory and experiment

Given the dramatic increase in power of computational methods over the last decade, it is now possible to routinely perform parallel theoretical calculations, and to examine which, if any, of the theoretical results are ambiguous and method-dependent, so that experimental information becomes crucial.

Upon initiating a theoretical calculation of a complex molecule one is confronted with a large number of choices of Hamiltonians and basis sets, which produce quantitatively different results, though the qualitative trends predicted are often robust and independent of method. In our calculations on the metastable states of the ruthenium–sulfur dioxide linkage isomers, for example, both smaller and larger basis set DFT calculations reveal, in addition to the observed (S,O) bound isomer, a third, non-yet observed, O-bound metastable state.¹¹ But this state is more stable than the ground state according to the smaller basis set calculation, an obviously unrealistic result that is corrected by the larger basis set.

From DFT calculations of the ground state of the $[\text{Pt}_2(\text{pyrophosphate})_4]^{4-}$ ion with the Amsterdam density functional (ADF) program package,³⁵ the spread between the various values for the Pt–Pt bond distance is ≈ 0.1 Å depending on the functional selected (B88LYP, B88P86, PW86LYP)[†] and the relativistic treatment adopted (Pauli or ZORA),³⁶ compared with an experimental standard deviation in each of the available analyses of less than 0.001 Å and a variation among the different solids of not more than 0.01 Å. Other bonds behave very much in the same manner. The local density approximation (LDA) with the functional of Vosko–Wilk–Nusair (VWN) was rejected,³⁷ as it produced too short Pt–Pt and Pt–P bonds and thus did not reproduce the ground state geometry satisfactorily. In addition to the geometry information from spectroscopy, EXAFS and diffraction, summarized above, spectroscopic energy differences are available for comparison with the theoretical results. The relative merits of the different calculations in reproducing the combined experimental information are depicted in Fig. 5, which shows the variation in Pt–Pt and Pt–P bond lengths and the excitation energy as predicted by different calculations and measured experimentally. The wide spread among the theoretical values for both the Pt–Pt shortening ($\Delta d \approx -0.2$ to -0.5 Å) and the excitation energy ($\Delta E \approx 1.9$ – 3.2 eV) is evident. The Pt–P bond length is invariably calculated to be larger in the excited state. This is intuitively acceptable, as a strengthening of the Pt–Pt interaction may be accompanied by a weakening of the other bonds to Pt, but is contrary to the EXAFS results, which have to be re-examined. As the ZORA FC PW86LYP gives reasonable results for both the Pt–Pt shortening and the ΔSCF excitation energy, it has been selected for the calculation of excited-state properties which are not accessible experimentally, such as the frontier molecular orbitals (Fig. 6), the charge density in the molecule, topological properties in the Pt–Pt bonding region, and the spin density in the excited state. The spin density is related to the high chemical reactivity of the excited state, which includes abstraction of hydrogen and chlorine atoms from a range of organic substrates, including DNA.³⁸

[†] The valence atomic orbitals of platinum, oxygen, phosphorus and hydrogen atoms were described by triple- ζ Slater-type basis sets with one polarization function added on the O, P and H atoms (ADF database IV). Relativistic effects were taken into account using either of two methods implemented in ADF: a quasi-relativistic method which employs the Pauli Hamiltonian and the zero order regular approximation (ZORA). The $(1s2s2p)^{10}$ and $(1s)^2$ shells of P and O, respectively, were treated by the frozen core (FC) approximation in all calculations. The $(1s2s2p3s3p4s3d4p4d)^{46}$ core shells of Pt were either kept frozen or *all* electrons of Pt (with the ZORA formalism) were used in the computation in which case the core was described by double- ζ quality basis set (the Pt all-electron calculations are labeled AE_{Pt} in the text).

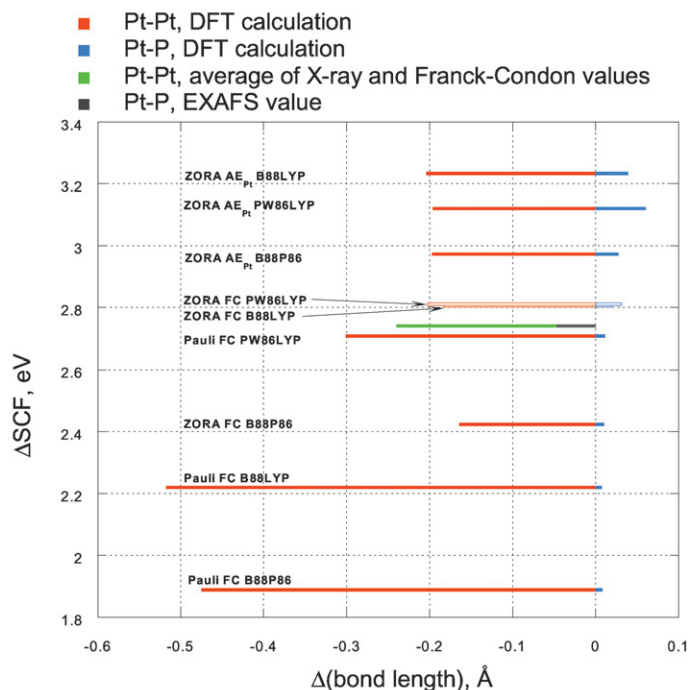


Fig. 5 Summary of theoretical and experimental Pt–Pt and Pt–P bond length changes and excitation energies for the $[\text{Pt}_2(\text{pyrophosphate})_4]^{4-}$ ion. Red bar: theoretical Pt–Pt bond shortening, blue bar: theoretical Pt–P bond length change, vertical axis: energy of excitation, green bar: average of X-ray and Franck–Condon values for Pt–Pt bond shortening and grey bar: EXAFS results for Pt–P bond change.

The calculation shows the spin density to be mostly located on the Pt atoms, which are the likely reactive sites.³⁶

A theoretical prediction of an excited state distortion

The tetrahedrally coordinated Cu(I) complexes distort towards a more planar geometry upon metal-to-ligand-charge-transfer (MLCT). A prototype example is Cu(I)bis(1,10-phenanthroline),^{39–41} the excited state distortion of which, and thereby its lifetime and other photophysical properties, can be manipulated by variation of the 2,9-substituents. The Cu bisphenanthrolines absorb light in the visible spectral region, and may show intense long-lifetime luminescence. In solution the luminescence tends to be quenched by exciplex formation, even with weak Lewis bases, but this cannot occur in the solid state, unless solvent molecules can be included with the guest in one cavity of a supramolecular solid, a possible avenue for investigation. Changes in coordination of the Cu atom upon excitation in solution have now been measured by EXAFS.¹⁸ Full information on the geometry changes is not yet available, but the geometry can be calculated for the isolated molecule. Calculations of Cu(I) bis(2,9-dimethyl-1,10-phenanthroline) cation with the ADF2002.01 program[‡],³⁵ indicate a flattening of the complex (Fig. 7), with the dihedral angle

[‡] DFT calculations were performed using the VWN local density functional and the gradient-corrected B88LYP functional. The copper atom was described by a triple- ξ basis set (ADF database “TZP”), the C, N and H atoms were described by double- ξ basis set augmented by one polarization function (ADF database “DZP”). The (1s2s2p) core shell of Cu and (1s) core shell of C and N were treated by the frozen core approximation. Relativistic effects were taken into account using the ZORA formalism. The calculations were symmetry-restricted to the D_2 point group.

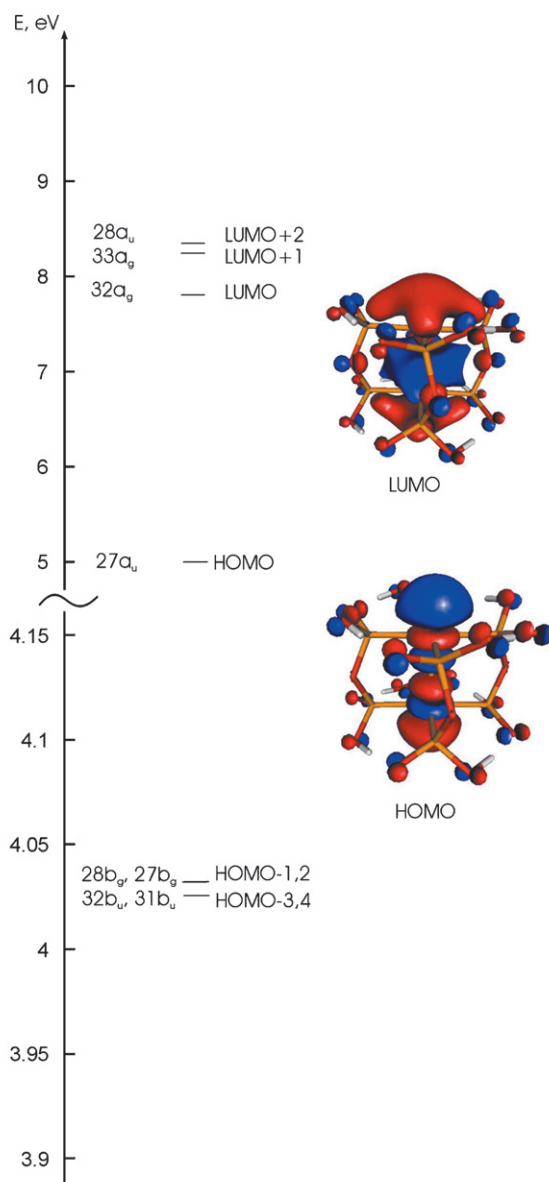


Fig. 6 Ordering of the frontier molecular orbitals in the ground state of $[\text{Pt}_2(\text{pyrophosphate})_4]^{4-}$ ion (ref. 36) Plotted isosurface value 0.025 a.u. Orbital designations refer to the C_{2h} point group.

between the phenanthroline planes decreasing from ≈ 80 to $\approx 65^\circ$ and a shortening of the Cu–N distances by $\sim 0.04 \text{ \AA}$ on MLCT.

This is in agreement with the predicted distortion from the essentially tetrahedral \S geometry of the ground state. Calculations of an exciplex with five-coordination of the Cu atom are now being pursued and will be reported separately.⁴²

\S The distortion of the ground state from the perfect tetrahedral geometry is due to the limiting N \cdots N chelate bite size, which restricts the N–Cu–N angles.

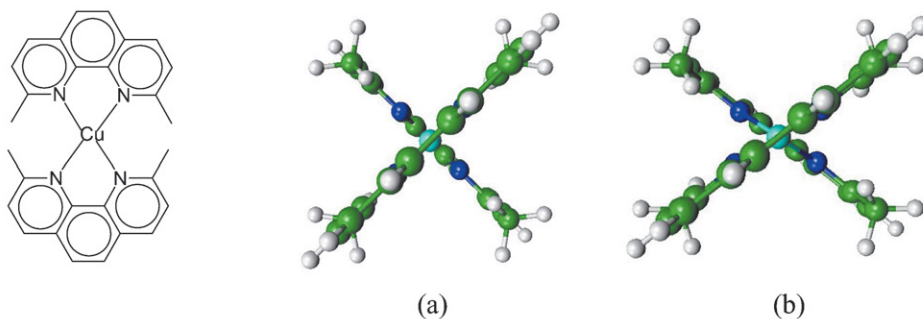


Fig. 7 Ground (a) and excited (b) state structure of Cu(I)bis(2,9-dimethyl 1,10-phenanthroline).

Concluding remarks

The interplay between theory and experiment is an essential component of time-resolved studies at atomic resolution. The combined approach opens a way for resolving theoretical as well as experimental ambiguities and for selecting the most reliable theoretical treatments for calculation of other quantities, such as molecular orbitals and excited state spin and charge densities, which are not experimentally accessible but are important for understanding excited-state properties. In future work non-reversible chemical reaction should attract increased attention as experimental methods are becoming more sophisticated and photon sources more powerful. The increasing application of theory to the study of mechanisms of chemical reactions,⁴³ should be a further impetus for collaboration between experimentalists and theoreticians.

Finally, notwithstanding the significant progress evident from what is presented in this issue, time-resolved chemistry at atomic resolution is still in its infancy, but will undoubtedly become a major research topic in the coming years.

Acknowledgements

Financial support of our work by the National Science Foundation (CHE9981864) and the Petroleum Research Fund of the American Chemical Society (PRF32638-AC3 and PRF37614-AC3) is gratefully acknowledged. The computations reported were performed on the 64-processor SGI Origin3800, 32-processor Sun Blade 1000 (UltraSparc III) and 48-processor Sun Ultra-5 (UltraSparc II) supercomputers at the Center for Computational Research of the State University of New York at Buffalo, which is supported by grant (DBI9871132) from the National Science Foundation.

References

- 1 A. H. Zewail, *J. Phys. Chem. A*, 2000, **104**, 5660.
- 2 F. Meneau, G. Sankar, N. Morgante, R. Winter, C. R. Catlow, G. N. Greaves and J. M. Thomas, *Faraday Discuss.*, 2002, **122**, 203.
- 3 E. L. Heeley, C. K. Poh, L. Wu, A. Maidens, W. Bras, I. P. Dolbnya, A. J. Gleeson, N. J. Terrill, J. Patrick, A. Fairclough, P. D. Olmstead, R. I. Ristic, M. J. Hounslow and A. J. Ryan, *Faraday Discuss.*, 2002, **122**, 343.
- 4 R. I. Walton, A. Norquist, R. I. Smith and D. O'Hare, *Faraday Discuss.*, 2002, **122**, 331.
- 5 See for example P. Norby, *J. Appl. Crystallogr.*, 1997, **30**, 21.
- 6 Z. Ren, B. Perman, V. Srajer, T.-Y. Teng, C. Pradervand, D. Bourgeois, F. Schotte, T. Ursby, O. R. Kort, M. Wulff and K. Moffat, *Biochemistry*, 2001, **40**, 13 788.
- 7 V. Srajer, Z. Ren, T.-Y. Teng, M. Schmidt, T. Ursby, D. Bourgeois, C. Pradervand, W. Schildkamp, M. Wulff and K. Moffat, *Biochemistry*, 2001, **40**, 13 802.
- 8 R. Helliwell, Y. P. Hieh, J. Habash, P. F. Faulder, J. Raftery, M. Cianci, M. Wulff and A. Hädener, *Faraday Discuss.*, 2002, **122**, 131.
- 9 G. Busse, T. Tschentscher, A. Plech, M. Wulff, B. Frederichs and S. Techert, *Faraday Discuss.*, 2002, **122**, 13.

- 10 P. Coppens, I. V. Novozhilova and A. Y. Kovalevsky, *Chem. Rev.*, 2002, **102**, 861.
- 11 A. Y. Kovalevsky, K. A. Bagley and P. Coppens, *J. Am. Chem. Soc.*, 2002, **124**, 9241.
- 12 I. Schlichting, J. Berendzen, K. Chu, A. M. Stock, S. A. Maves, D. E. Benson, R. M. Sweet, D. Ringe, G. A. Petsko and S. G. Sligar, *Science*, 2000, **287**, 1615.
- 13 T. C. Brunold and H. U. Gudel, in *Inorganic Electronic Structure and Spectroscopy, Volume I: Methodology*, ed. E. I. Solomon and A. B. P. Lever, Wiley, New York, 1999, p. 259.
- 14 J. I. Zink, *Coord. Chem. Rev.*, 2001, **21**, 69.
- 15 S. E. Bailey, R. E. Eikey, M. M. Abu-Omar and J. I. Zink, *Inorg. Chem.*, 2002, **41**, 1755.
- 16 X. Z. Sun, M. W. George, S. G. Kazarian, S. M. Nikiforov and M. Poliakoff, *J. Am. Chem. Soc.*, 1996, **118**, 10525.
- 17 L. X. Chen, W. J. H. Jager, G. Jennings, D. J. Gosztola, A. Munkholm and J. P. Hessler, *Science*, 2001, **292**, 262.
- 18 L. X. Chen, *Faraday Discuss.*, 2002, **122**, 315.
- 19 J. Cao, H. Ihee and A. H. Zewail, *Proc. Natl. Acad. Sci. USA*, 1999, **96**, 338.
- 20 R. C. Dudek and P. M. Weber, *J. Phys. Chem. A*, 2001, **105**, 4167.
- 21 P. Coppens, B. Ma, O. Gerlits, Y. Zhang and P. Kulshrestha, *CrystEngComm*, 2002, **4**, 302.
- 22 W. Schuddeboom, S. A. Jonker, J. M. Warman, U. Leinhos, W. Kuhnle and K. A. Zachariasse, *J. Phys. Chem.*, 1992, **96**, 10809.
- 23 H. Okamoto, *J. Phys. Chem. A*, 2000, **104**, 4182.
- 24 W. M. Kwok, C. Ma, P. Matousek, A. W. Parker, D. Phillips, W. T. Toner, M. Towrie and S. Umaphathy, *J. Phys. Chem. A*, 2001, **105**, 984.
- 25 S. Techert, F. Schotte and M. Wulff, *Phys. Rev. Lett.*, 2001, **86**, 2030–2033.
- 26 C. Ma, W. M. Kwok, P. Matousek, A. W. Parker, D. Phillips, W. T. Toner and M. Towrie, *J. Phys. Chem. A*, 2001, **105**, 4684.
- 27 (a) A. E. Stiegman, S. F. Rice, H. B. Gray and V. M. Miskowski, *Inorg. Chem.*, 1987, **26**, 1112; (b) S. F. Rice and H. B. Gray, *J. Am. Chem. Soc.*, 1983, **105**, 4571.
- 28 J. T. Markert, D. P. Clements and M. R. Corson, *Chem. Phys. Lett.*, 1983, **97**, 175.
- 29 L. Ribaud, G. Wu, Y. Zhang and P. Coppens, *J. Appl. Crystallogr.*, 2001, **34**, 76.
- 30 S. F. Rice and H. B. Gray, *J. Am. Chem. Soc.*, 1983, **105**, 4571.
- 31 P. Stein, M. K. Dickson and D. M. Roundhill, *J. Am. Chem. Soc.*, 1983, **105**, 3489.
- 32 D. J. Thiel, P. Liviš, E. A. Stern and A. Lewis, *Nature*, 1993, **362**, 40.
- 33 M. D. Carducci, M. R. Pressprich and P. Coppens, *J. Am. Chem. Soc.*, 1997, **119**, 2669.
- 34 Y. Ozawa, M. R. Pressprich and P. Coppens, *J. Appl. Crystallogr.*, 1998, **31**, 128.
- 35 (a) E. J. Baerends, D. E. Ellis and P. Ros, *Chem. Phys.*, 1973, **2**, 41; (b) L. Versluis and T. Ziegler, *J. Chem. Phys.*, 1988, **88**, 322; (c) G. te Velde and E. J. Baerends, *J. Comput. Phys.*, 1992, **99**, 84; (d) C. Fonseca Guerra, J. G. Snijders, G. te Velde and E. J. Baerends, *Theor. Chem. Acc.*, 1998, **99**, 391.
- 36 I. V. Novozhilova, A. Volkov and P. Coppens, manuscript in preparation.
- 37 S. H. Vosko, L. Wilk and M. Nusair, *Can. J. Phys.*, 1980, **58**, 1200.
- 38 D. M. Roundhill, H. B. Gray and C. M. Che, *Acc. Chem. Res.*, 1989, **22**, 55.
- 39 P. A. Breddels, P. A. M. Berdowski, G. Blasse and D. R. McMillin, *J. Chem. Soc., Faraday Trans.*, 1972, **78**, 595.
- 40 D. V. Scaltrito, D. W. Thompson, J. A. O'Callaghan and G. J. Meyer, *Coord. Chem. Rev.*, 2000, **208**, 243.
- 41 N. Armaroli, *Chem. Soc. Rev.*, 2001, **30**, 113.
- 42 I. V. Novozhilova and P. Coppens, manuscript in preparation.
- 43 (a) A. Michalak and T. Ziegler, *J. Am. Chem. Soc.*, 2001, **123**, 12266; (b) E. Zurek and T. Ziegler, *Organometallics*, 2002, **21**, 83.